

Simulation of femtosecond laser ablation of silicon

Roman Holenstein^a, Robert Fedosejevs^a, Ying Y. Tsui^a, Sean E. Kirkwood^a

^aDept. of Electrical Engineering, University of Alberta, Edmonton, Canada

ABSTRACT

Femtosecond laser ablation is an important process in the micromachining and nanomachining of microelectronic, optoelectronic, biophotonic and MEMS components. The process of laser ablation of silicon is being studied on an atomic level using molecular dynamics (MD) simulations. We investigate ablation thresholds for Gaussian laser pulses of 800 nm wavelength, in the range of a few hundred femtoseconds in duration. Absorption occurs into a hot electron bath which then transfers energy into the crystal lattice. The simulation box is a narrow column approximately 5.4 nm x 5.4 nm x 81 nm with periodic boundaries in the x and y transverse directions and a 1-D heat flow (HF) model at the bottom coupled to a heat bath to simulate an infinite bulk medium corresponding to the solid bulk material. A modified Stillinger-Weber potential is used to model the silicon atoms. The calculated thresholds are compared to various reported experimental values for the ablation threshold of silicon. We provide an overview of the code and discuss the simulation techniques used.

Keywords: Laser ablation, silicon, molecular dynamics, near-IR, ultrafast

1. INTRODUCTION

Recent advances in ultrafast lasers have made them an attractive tool for micromachining. Due to the commercial availability of ultrafast solid state lasers in the last few years, ultrafast laser ablation has found many applications in industry and medicine. Examples of these include fabrication and repair of microelectrical mechanical systems (MEMS), microchannels for fluidic devices, and isolating features for electrical microchips.

The dominant mechanisms involved in ultrafast laser ablation are different from long-pulse ablation. While ablation on a longer time scale (nanoseconds or longer) are reasonably well understood, the physics involved in ablation using ultrashort (picosecond, femtosecond) pulse lengths are not yet fully understood. There have been many attempts in the past decade to explain the relevant processes, both theoretical¹⁻³ and experimental.⁴⁻⁷

Computer simulations are often used to gain insight in the mechanism involved in a particular phenomena. Using simulations it is possible to isolate different processes and assess their contribution, which is much more difficult or often even impossible in experiments. Molecular dynamics (MD) simulations have already been used to model laser-matter interaction for various materials, including metals,⁸ organic solids,⁹ and semiconductors.¹⁻³

2. SIMULATION MODEL

We employ molecular dynamics simulations to model the ablation process. In MD the physical system is represented as a number of particles (e.g. atoms), the trajectories of which are computed using Newtonian mechanics. A Gear's 5th-order predictor-corrector algorithm was used to integrate the equations of motion.¹⁰

Further author information: (Send correspondence to R.F.)

R.H.: E-mail: roman@ece.ualberta.ca

R.F.: E-mail: rfed@ece.ualberta.ca

Y.Y.T.: E-mail: tsui@ece.ualberta.ca

S.E.K.: E-mail: kirkwood@ece.ualberta.ca

2.1. Particle interaction

The interactions between the silicon particles was modelled using the Stillinger-Weber (SW) potential¹¹ with the parameters given by Balamane et al.¹² The SW potential has 2-body and 3-body interactions. The 2-body term is of the form

$$V_2(r) = (A_1 r^{-4} - A_2) \exp\left[\frac{\sigma}{r-a}\right] \quad (1)$$

where $a = 3.77 \text{ \AA}$ is the cutoff distance, $A_1 = 189.36 \text{ eV \AA}^4$ and $A_2 = 16.32 \text{ eV}$ are constants. The 3-body term consists of exponential functions and an angular term, favouring the diamond lattice structure:

$$V_3(r_{ij}, r_{ik}, \theta_{jik}) = \lambda \exp\left(\frac{\gamma\sigma}{r_{ij}-a}\right) \exp\left(\frac{\gamma\sigma}{r_{ik}-a}\right) \left(\cos\theta_{jik} + \frac{1}{3}\right)^2 \quad (2)$$

r_{ij} and r_{ik} are the distances between the particles, θ_{jik} is the bonding angle, and $\lambda = 48.61 \text{ eV}$.

2.2. Setup

The initial bulk was 5.4 nm in width (x,y direction) and 81 nm in height (z), with periodic boundary conditions in x and y. 120000 atoms were used in the simulation. The MD system was coupled to a 1-D heat flow (HF) model at the bottom. The HF system was connected to a heat bath set to 300 K, to simulate an infinite bulk medium.

The step size was set to 0.5 fs. The lattice was initialised to $T_0 = 300$ Kelvin by setting the initial atomic velocities to a Maxwell-Boltzmann distribution. For the first 400 time steps the particles were damped to T_0 , followed by a relaxation period of 800 fs. The laser pulse was Gaussian in time and set in at $t = 1$ ps, with a peak intensity at $t = 1 \text{ ps} + \tau_L/2$, where τ_L is the pulse width (1/e).

2.3. Coupling of HF and MD system

The MD and HF system were energetically coupled as illustrated in figure 1. A section at the bottom of the MD system overlaps with the top of the heat flow system. The MD particles in the bottom region (~ 4 nm) are damped to the temperature obtained from the HF model. The damping was done using Langevin dynamics.^{13,14} The force on the atoms is given by

$$m_k \ddot{\vec{r}}_k = \vec{F}_k(\vec{r}_1, \dots, \vec{r}_N) - m_k \gamma \dot{\vec{r}}_k + \vec{R}_k \quad (3)$$

where $\gamma_k = \pi k_B \theta_D / (6\hbar)$ and $\vec{R}_k = \sqrt{2\gamma_k k_B T m_k} \vec{\eta}_k$ are random white noise forces. $\vec{\eta}_k$ are vectors of Gaussian random numbers centered at zero and $\theta_D = 645 \text{ K}$ is the Debye temperature of Si.

Similarly, the energy flux from the MD to the HF system is determined from Langevin dynamics. Assuming that the contributions to the velocity of the MD particles due to the random forces \vec{R}_k are small (the time steps are sufficiently small), the energy transfer into the HF system is:

$$\frac{\langle \Delta E \rangle}{\Delta t} = 3\gamma_k k_B (T_{\text{MD}} - T_{\text{HF}}) \quad (4)$$

where $\langle \Delta E \rangle$ the energy transferred per time step Δt , T_{MD} and T_{HF} are the (average) temperature in the molecular dynamics and heat flow regions as indicated in figure 1.

The coupling was tested by simulating a surface heat source. The surface atoms were continually ‘‘damped’’ to 1200 Kelvin. The temperature evolution of the system is shown in figure 2. The top portion above the horizontal line represents the temperature profile of the molecular dynamics system, and below the line is the heat flow system. We can see that the energy is coupled into the HF system, although a small ‘‘kink’’ is visible in the iso-therms. This is due to a small mismatch in the heat capacity and heat conductivity. Overall the coupling performs sufficiently and is adequate.

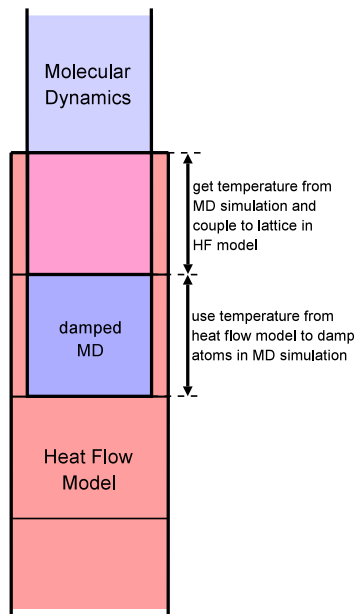


Figure 1. Molecular Dynamics-Heat Flow hybrid model: layout of interfacing.

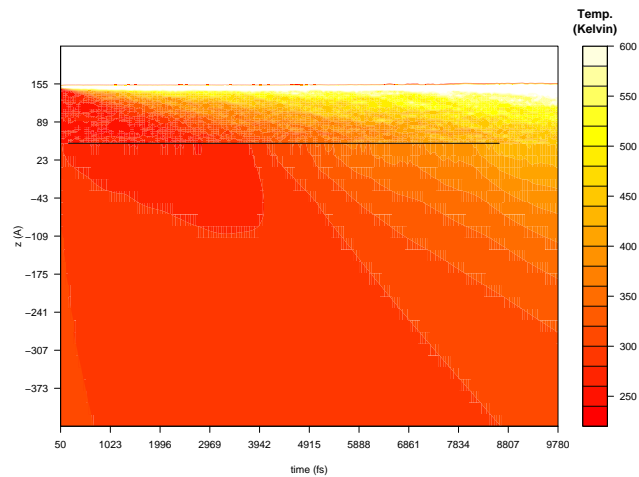


Figure 2. Evolution of temperature profile under continuous heating of the surface. The horizontal black line indicates the boundary between the MD system (above) and the HF system (below).

2.4. Laser absorption

The laser beam entered the system from the top. For this study, using ultrafast pulses in the near-infrared, linear and two-photon absorption are assumed to be the dominant absorption mechanisms.^{1, 15, 16} The number of photons entering the system in a given time step is determined. These are then traversed down the system, and each photon has a probability of being absorbed any of the encountered atoms. The linear and two-photon absorption coefficients are $\alpha = 803.45 \text{ cm}^{-1}$ and $\beta = 55 \text{ cm/GW}$, respectively.^{17, 18} After an atom had absorbed a photon, it was marked as an excited atom, that is, its excitation level was incremented. This represents the generation of “quasi-free” carriers, as suggested by von der Linde et al.,¹⁵ which then thermalize on a time scale of about 10^{-14} s. The excited electrons decay (couple to the phonon modes) on a time scale of 10^{-12} s. The released energy was added to a random atom within 3.8 \AA . An excitation changes the electronic structure of an atom, and thus the interaction with other particles. This was implemented by randomly breaking a number of bonds matching the excitation level.^{1, 16} Since Si has four valence electrons, an atom at 4th excitation was considered unbound. A broken bond was simulated by removing the attractive part of the two-body potential and discarding the three-body part of the SW potential.¹

If after repeated absorption the total energy absorbed exceeds the workfunction, 4.85 eV for Si, then the atom was ionised. A free electron was added to the system, the excitation level reset to zero, and the level of ionisation incremented. The electron was released with a velocity in a direction away from the ejecting Si particle at a distance of 1.17 \AA , which is half the nearest neighbour distance in the initial diamond lattice. The charged particles interacted through the Coulomb potential. For the ions, the Coulomb potential was in addition to the SW potential. A cutoff distance of 20 \AA was used, which was found to be sufficient.¹ An electron can recombine with an ion if it passes within 1 \AA of the ion. The ions are given a lifetime of 500 fs, which is to account for recombination with electrons supplied from the bulk.

3. RESULTS AND DISCUSSION

Simulations were carried out for single laser pulses at a wavelength of $\lambda = 800 \text{ nm}$. The pulse length was varied from 50 fs to 800 fs.

3.1. Ablation

Figure 3 shows a series of frames illustrating the process of matter removal using a laser pulse with fluence just above the threshold for ablation. The pulse length used in the displayed simulation was 100 fs and the fluence was 100 fs. The particles are coloured according to their coordination number (CN). Solid silicon has a coordination number of 4. As the material melts, the CN rises to about 5-6.^{19, 20} We can see the nucleation of a bubble within the melted region.

3.2. Thresholds

We obtained the melting and ablation thresholds for pulse length on the order of 10^{-13} s. For each pulse length the fluence was varied in steps of $0.01 - 0.02 \text{ J/cm}^2$. The ablation thresholds were determined by examining the simulations both visually (e.g. see figure 3) and in terms of number of removed atoms. The threshold was taken as the median between the lowest fluence giving clearly visible ablation (F_{abs}^+) and the highest fluence giving resulting in no ablation (F_{abs}^-). The error bars indicate the range between F_{abs}^- and F_{abs}^+ . With the fluence increments used, ablation set in suddenly and clearly. With smaller increments, a better definition for the threshold may be required, however, for now the current one is sufficient. The melting threshold was estimated as the minimum fluence required to heat the surface above to the melting temperature of Si. The threshold fluences for melting and ablation are given in table 1.

In figure 4 we compare our results with reported theoretical and experimental values from the literature. There is a large variation in the reported values, which is due to different experimental conditions. In order to compare the data from different groups, we have presented the thresholds in absorbed fluence, taking into account reflectivity,[?] polarisation and angle of incidence where possible (e.g. Cavalleri et al.⁵). The results by Jeschke, which are given in terms of absorbed energy per atom, have been converted to an absorbed fluence by considering an effective 2-photon absorption skin depth ($\beta = 55 \text{ cm/GW}$). We have approximate agreement or

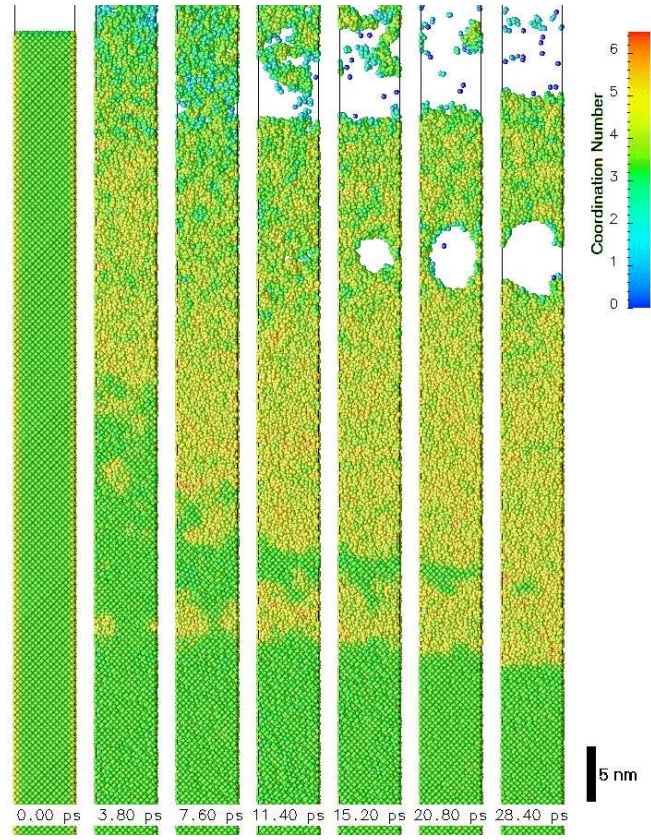


Figure 3. Ablation sequence for 100 fs laser pulse with a fluence of 0.16 J/cm^2 ($\lambda = 800 \text{ nm}$). The laser pulse starts at $t = 1 \text{ ps}$ with peak intensity at $t = 1.1 \text{ ps}$

τ_L [fs]	$F_{\text{abs}}^{[m]}$ [$\frac{\text{J}}{\text{cm}^2}$]	$F_{\text{abs}}^{[a]}$ [$\frac{\text{J}}{\text{cm}^2}$]
50	0.07 ± 0.01	0.09 ± 0.01
100	< 0.10	0.13 ± 0.02
200	< 0.16	0.19 ± 0.02
400	-	0.26 ± 0.03
800	0.39 ± 0.03	-

Table 1. Threshold absorbed fluences for melting ($F_{\text{abs}}^{[m]}$) and ablation ($F_{\text{abs}}^{[a]}$). Some of the thresholds have not been established yet and further simulations are required.

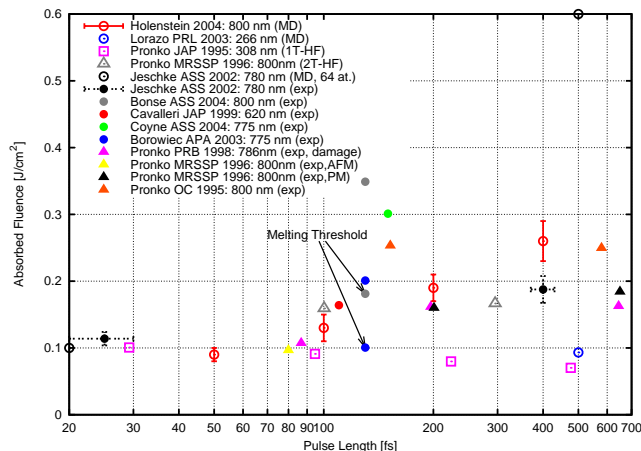


Figure 4. Single shot ablation thresholds compared to literature values at different pulse lengths over the range of 20 fs to 700 fs.^{2-7,21-23} Presented are absorbed fluences, taking into account reflectivity, polarisation and angle of incidence where applicable. The filled symbols represent experimental results and the open ones are from theoretical studies.

our calculated ablation threshold, $F_{\text{abs}}^{[a]} = 0.13 \text{ J/cm}^2$, at 100 fs with experimental values. The MD results at longer pulse lengths, however, start to deviate from the experimental data.

4. SUMMARY

The process of ultrafast laser ablation of Si was simulated using molecular dynamics and 1-D heat diffusion model. An coupling mechanism based on Langevin dynamics was used to the HF and MD systems. The threshold fluences for matter removal were estimated for several pulse lengths between 50 fs and 400 fs at a wavelengths of 800 nm. The threshold fluences were comparable to experimental values, however, our results showed a stronger pulse length scaling. Further simulations are required to test a wider range of pulse lengths. Also, the effects of avalanche ionisation are not yet included in our simulations and need to be investigated, as it may be a significant factor in the absorption mechanism and consequently affect the ablation process and threshold values.⁴

ACKNOWLEDGMENTS

We acknowledge financial support by the Canadian Institute for Photonic Innovations (CIPI), the National Sciences and Engineering Research Council of Canada (NSERC), and the Informatics Circle of Research Excellence (iCore). Computational support for this work was provided by the WestGrid project.

REFERENCES

1. R. Herrmann, J. Gerlach, and E. Campbell, “Ultrashort pulse laser ablation of silicon: an md simulation study,” *Appl. Phys. A* **66**, p. 35, 1998.
2. H. Jeschke, M. Garcia, M. Lenzner, J. Bonse, J. Krüger, and W. Kautek, “Laser ablation thresholds of silicon for different pulse durations: theory and experiment,” *Appl. Surf. Sci.* **197-198**, pp. 839–844, 2002.
3. P. Lorazo, L. Lewis, and M. Meunier, “Short-pulse laser ablation of solids: From phase explosion to fragmentation,” *Phys. Rev. Lett.* **91**, p. 225502, 2003.
4. P. Pronko, P. VanRompay, C. Horvth, F. Loesel, T. Juhasz, X. Liu, and G. Mourou, “Avalanche ionization and dielectric breakdown in silicon with ultrafast laser pulses,” *Phys. Rev. B* **58**, p. 2387, 1998.
5. A. Cavalleri, K. Sokolowski-Tinten, J. Bialkowski, M. Schreiner, and D. von der Linde, “Femtosecond melting and ablation of semiconductors studied with time of flight mass spectroscopy,” *J. Appl. Phys.* **85**, p. 3301, 1999.

6. A. Borowiec, M. MacKenzie, G. Weatherly, and H. Haugen, "Transmission and scanning electron microscopy studies of single femtosecond-laser-pulse ablation of silicon," *Appl. Phys. A* **76**, p. 201, 2003.
7. J. Bonse and A. M. K.-W. Brzezinka, "Modifying single-crystalline silicon by femtosecond laser pulses: an analysis by micro raman spectroscopy, scanning laser microscopy and atomic force microscopy," *Appl. Surf. Sci.* **221**, p. 215, 2004.
8. D. Ivanov and L. Zhigilei, "Effect of pressure relaxation on the mechanisms of short-pulse laser melting," *Phys. Rev. Lett.* **91**, p. 105701, 2003.
9. L. Zhigilei, E. Leveugle, B. Garrison, Y. Yingling, and M. Zeifman, "Computer simulations of laser ablation of molecular substrates," *Chem. Rev.* **103**, p. 321, 2003.
10. J. Haile, *Molecular Dynamics Simulation: Elementary Methods*, John Wiley & Sons, Inc., New York, 1997.
11. F. Stillinger and T. Weber, "Computer simulation of local order in condensed phases of silicon," *Phys. Rev. B* **31**, p. 5262, 1985.
12. H. Balamane, T. Halicioglu, and W. Tiller, "Comparative study of silicon empirical interatomic potentials," *Phys. Rev. B* **46**, p. 2250, 1992.
13. S. Adelman and J. Doll, "Generalized langevin equation approach for atom/solid-surface scattering: General formulation for classical scattering off harmonic solids," *J. Chem Phys.* **64**, p. 2375, 1976.
14. H. Haberland, Z. Insepov, and M. Moseler, "Molecular-dynamics simulation of thin-film growth by energetic cluster impact," *Phys. Rev. B* **51**, p. 11061, 1995.
15. D. Von der Linde, K. Sokolowski-Tinten, and J. Bialkowski, "Laser-solid interaction in the femtosecond time regime," *Appl. Surf. Sci.* **109-110**, p. 1, 1997.
16. P. Stampfli and K. Bennemann, "Time dependence of the laser-induced femtosecond lattice instability of si and gaas: Role of longitudinal optical distortions," *Phys. Rev. B* **49**, p. 7299, 1994.
17. D. Aspnes and A. Studna, "Dielectric functions and optical parameters of si, ge, gap, gaas, gasb, inp, inas, and insb from 1.5 to 6 eV," *Phys. Rev. B* **27**, p. 985, 1983.
18. K. Sokolowski-Tinten, J. Bialkowski, and D. von der Linde, "Ultrafast laser-induced order-disorder transitions in semiconductors," *Phys. Rev. B* **51**, p. 14186, 1995.
19. Y. Waseda and K. Suzuki, "Structure of molten silicon and germanium by x-ray diffraction (and calculation of resistivity and thermoelectric power)," *Z. Phys. B* **20**, p. 339, 1975.
20. J. Gabathuler and S. Steeb, "[title]," *Z. Naturforsch. A* **34**, p. 1314, 1979.
21. P. Pronko, S. Dutta, D. Du, and R. Singh, "Thermophysical effects in laser processing of materials with picosecond and femtosecond pulses," *J. Appl. Phys.* **78**, p. 6233, 1995.
22. E. Coyne, J. Magee, P. Mannion, G. O'Connor, and T. Glynn, "Characterization of laser ablation of silicon using a gaussian wavefront and computer generated wavefront reconstruction," *Appl. Surf. Sci.* **229**, pp. 148-160, 2004.
23. P. Pronko, P. VanRompay, R. Singh, F. Qian, D. Du, and X. Liu, "Laser induced avalanche ionization and electron-lattice heating of silicon with intense near ir femtosecond pulses," in *Mat. Res. Soc. Symp. Proc.*, **397**, p. 45, 1996.